Volume 56(8): 753–764, 2008
Journal of Histochemistry & Cytochemistry
http://www.jhc.org

ARTICLE

Periostin Is Expressed in Pericryptal Fibroblasts and Cancer-associated Fibroblasts in the Colon

Yoshinao Kikuchi, Takeshi G. Kashima, Takashi Nishiyama, Kazuhiro Shimazu, Yasuyuki Morishita, Masashi Shimazaki, Isao Kii, Hisanaga Horie, Hideo Nagai, Akira Kudo, and Masashi Fukayama

Department of Pathology and Diagnostic Pathology, Graduate School of Medicine, The University of Tokyo, Tokyo, Japan (YK,TGK,KS,YM,MF); Department of Biological Information, Tokyo Institute of Technology, Yokohama, Japan (TN,MS, IK,AK); Department of Surgery, Jichi Medical School, Tochigi, Japan (HH,HN); and Ibaraki Prefectural Central Hospital, Ibaraki, Japan (HN)

SUMMARY Periostin is a unique extracellular matrix protein, deposition of which is enhanced by mechanical stress and the tissue repair process. Its significance in normal and neoplastic colon has not been fully clarified yet. Using immunohistochemistry and immunoelectron microscopy with a highly specific monoclonal antibody, periostin deposition was observed in close proximity to pericryptal fibroblasts of colonic crypts. The pericryptal pattern of periostin deposition was decreased in adenoma and adenocarcinoma, preceding the decrease of the number of pericryptal fibroblasts. Periostin immunoreactivity appeared again at the invasive front of the carcinoma and increased along the appearance of cancer-associated fibroblasts. ISH showed periostin signals in cancer-associated fibroblasts but not in cancer cells. Ki-67–positive epithelial cells were significantly decreased in the colonic crypts of periostin$^{-/-}$ mice ($\sim$0.6-fold) compared with periostin$^{+/+}$ mice. In three-dimensional coculture within type I collagen gel, both colony size and number of human colon cancer cell line HCT116 cells were significantly larger ($\sim$1.5-fold) when cultured with fibroblasts derived from periostin$^{+/+}$ mice or periostin-transfected NIH3T3 cells than with those from periostin$^{-/-}$ mice or periostin–non-producing NIH3T3 cells, respectively. Periostin is secreted by pericryptal and cancer-associated fibroblasts in the colon, both of which support the growth of epithelial components. **(J Histochem Cytochem 56:753–764, 2008)**

KEY WORDS
periostin
pericryptal fibroblast
cancer-associated fibroblast
colon
adenoma–carcinoma sequence

PERIOSTIN is a unique extracellular matrix protein in the collagen-rich connective tissues, such as periodontal ligament, periosteum, fascia of skeletal muscles, and cardiac valve (Takeshita et al. 1993; Horiuchi et al. 1999; Kruzynska Frejtag et al. 2001; Hirose et al. 2003; Kruzynska Frejtag et al. 2004; Suzuki et al. 2004; Norris et al. 2007), and its deposition is augmented by the increase of mechanical pressure. Recently, we showed that periostin recruits activated fibroblasts and forms collagen fibrils in the healing process of acute myocardial infarction (Shimazaki et al. 2008). In the study of tissue distribution of the periostin molecule, we observed deposition of periostin in mouse and human colon in close proximity to the pericryptal fibroblast (PCF), a myofibroblast at the epithelial–mesenchymal interface surrounding the colonic crypts. The PCF is situated beneath the epithelial basal membrane and assumed to play a fundamental role in epithelial differentiation during fetal and adult life. PCF interacts with epithelial cells through regulating basement membrane molecules and secreting paracrine factors (Birchmeier and Birchmeier 1993; Kedinger et al. 1999; Naftalin and Pedley 1999; Powell et al. 1999; Spradling et al. 2001).

Periostin has also been shown in various neoplastic tissues, including cancers of the breast, pancreas, and colon (Sasaki et al. 2003; Bao et al. 2004; Shao et al. 2004; Tai et al. 2005; Grigoriadis et al. 2006; Baril et al. 2007), but the tissue distribution has been controversial. Periostin, when transfected to cancer cells, promotes tumor angiogenesis, metastatic growth, can-

Correspondence to: Masashi Fukayama, 7-3-1, Hongo, Bunkyo-ku, Tokyo 113-0033, Japan. E-mail: mfukayama-tky@umin.ac.jp
Received for publication February 4, 2008; accepted April 15, 2008 [DOI: 10.1369/jhc.2008.951061].

0022-1554/08/$3.30

cer cell motility, and adhesion (Gillan et al. 2002; Bao et al. 2004; Shao et al. 2004; Kudo et al. 2006; Yan and Shao 2006; Baril et al. 2007). Although most of these studies postulate cancer cells as a source of periostin, there have been unexpectedly few cancer cell lines that expressed significant amounts of periostin mRNA in vitro (Gillan et al. 2002; Bao et al. 2004; Yan and Shao, 2006) (unpublished data). It is also controversial which types of cells produce periostin in the neoplastic tissue by morphological studies. Baril et al. (2007) showed mRNA of periostin in cancer cells by ISH in pancreatic cancer. In contrast, strong expression of periostin mRNA was observed in cancer stromal cells in lung cancers and breast cancers (Sasaki et al. 2001,2003). Erkan et al. (2007) showed that stellate cells produced periostin in normal and neoplastic pancreas.

In this study, we investigated localization and function of periostin in non-neoplastic and neoplastic colon, with special attention to the PCF and the other type of myofibroblast, the cancer-associated fibroblast (CAF). Furthermore, functional studies, using periostin knockout mice, also showed growth-promoting function of periostin molecules.

Materials and Methods

Tissue Specimens

Tissue specimens consisted of non-neoplastic tissues of human colon including the biopsy specimens of ulcerative colitis (3 cases) and the neoplastic tissues; carcinoma in adenoma (16 cases), carcinoma with early invasion (8 cases) and advanced invasion (24 cases); and metastatic colon cancer of the liver (13 cases). All specimens were retrieved from the files of the Department of Diagnostic Pathology, University of Tokyo Hospital. According to the criteria of the Japanese Research Society for Cancers of the Colon and Rectum (Japanese Society for Cancer of the Colon and Rectum 2006), we regarded early carcinomas as those showing invasion to the submucosal layer and advanced invasive as colon cancers beyond the proper muscular layer. Tissue samples had been formalin fixed and embedded in paraffin for histopathological examination.

For the assessment of RT-PCR, frozen tissue samples of the carcinoma and non-neoplastic mucosa were obtained from the surgically resected colons for the treatment of the carcinomas at Jichi Medical School Hospital. These tissue specimens were immediately frozen and stored at –80C. Informed consent was obtained from each patient to allow the use of portions of tissue for research purposes, and the study was approved by the ethical committee of the institutions.

For the histological analysis of the colon of periostin$^{-/-}$ mice, we used three 12-week-old mice homozygous for the disrupted periostin gene (Kii et al. 2006; Shimazaki et al. 2008) and the same number of wild-type littermates.

Mice were treated in accordance with the policies of the Animal Ethics Committee of the University of Tokyo.

Cell and Culture

The colon cancer cell line HCT116, mouse fibroblast cell line NIH3T3, and periostin$^{+/+}$ or periostin$^{-/-}$ mouse lung primary-cultured fibroblasts were used for proliferation assay and/or colony formation assay. They were routinely grown in DMEM (Sigma; St. Louis, MO) with 10% FBS, 100 U/ml penicillin, and 100 μg/ml streptomycin, at 37C saturated with 5% CO_2 in a humid atmosphere. Primary-cultured lung fibroblasts derived from periostin$^{+/+}$ and periostin$^{-/-}$ mice were obtained by the digestion method with DISPASE I (GODO SHUSEI Co.; Tokyo, Japan) according to the manufacturer's instructions. These primary-cultured fibroblasts were used in experiments before the fifth passage.

Transfection

Expression vectors for mouse periostin with HA tag and enhanced green fluorescent protein (EGFP) were previously constructed in pCAGIPuro (Li et al. 1999) (kindly provided by Dr. H. Niwa, RIKEN Center for Developmental Biology, Kobe, Japan) (Kii I, et al., unpublished data). Cells were transfected by FuGene 6 Transfection Reagent (Roche Diagnostics; Indianapolis, IN) according to the manufacturer's instructions. Selection and cloning were performed using puromycin (Sigma).

Immunohistochemistry and Double Immunofluorescence

The primary antibodies used in this study were a rabbit polyclonal anti-human periostin antibody (Shimazaki et al. 2008), a mouse monoclonal anti-α smooth muscle actin (αSMA) (1A4, 1:50; DakoCytomation, Glostrup, Denmark), a rabbit polyclonal anti-single-strand DNA antibody (ssDNA, 1:100; DakoCytomation), and a rat monoclonal anti-mouse Ki-67 antibody (TEC-3, 1:50; DakoCytomation), FITC-conjugated monoclonal anti-αSMA (mouse monoclonal 1A4-FITC, 1:300; Sigma). For immunohistochemistry, antibody binding was visualized by the avidin-biotin complex technique using 3,3-diaminobenzidine (DAB) as the chromogen. For double immunofluorescence, binding of the periostin antibody was visualized by goat anti-rabbit IgG labeled with Alexa fluor 594 (Molecular Probes; Eugene, OR), and sections were mounted with 4′,6-diamidine-2′-phenylindole dihydrochloride (DAPI) for nuclear staining (Vectashield Hardset Mounting Medium with DAPI; Vector Labs, Burlingame, CA).

For the assessment of pericryptal immunoreactivity of the colonic crypts or tumor glands with semiquantification, we defined positive crypts or glands when all circumferences were surrounded by immunoreactive material. The population of positive crypts or glands was counted and scored in four groups according to prevalence: score 0, <10%; score 1, 10–49%; score 2, 50–80%; score 3, >80%.

Immunoelectron Microscopy

Normal mouse colon tissues of Jcl:MCH (ICR) mice, 10 weeks old (CLEA Japan; Tokyo, Japan), were fixed in 4% paraformaldehyde-phosphate buffer (pH 7.0) overnight at 4C and washed in a series of ascending concentrations from 10% to 15%, 20% sucrose in PBS each for 4 hr, and then immersed in 20% sucrose and 5% glycerol in PBS for 1 hr. The tissues were embedded in OCT compound and frozen. After frozen sections (8 μm thick) were cut in a cryostat, primary antibody and secondary antibody were applied, and antibody binding was visualized by DAB as described above. They were then embedded in Epon 812. For light microscopic analysis, semithin sections (1 μm) were stained with toluidine blue. For immunoelectron microscopy, ultrathin sections were contrasted only with uranyl acetate omitting the staining of lead citrate and examined with an electron microscope (Model 1200EX; JEOL, Tokyo, Japan).

ISH for Periostin mRNA

Antisense and sense cRNA probes were prepared by in vitro transcription of the EcoRI-XbaI fragment of human periostin cDNA (Accession number D13665) (Takeshita et al. 1993), using a DIG Labeling MIX (Roche; Indianapolis, IN). The mRNA ISH was conducted according to the manufacturer's instructions (Roche).

Quantitative Periostin mRNA Real-time RT-PCR

Total RNA was isolated by the acid guanidine-thiocyanate/phenol/chloroform method or RNeasy Mini Kit (Qiagen; Valencia, CA). Reverse transcription was performed using Ready To Go 1st strand cDNA kit (GE Healthcare Bio-Sciences; Uppsala, Sweden).

For the quantitative periostin real-time RT-PCR, the housekeeping gene, *β-actin*, was used as an internal reference. The sequences of the primer sets were as follows: human periostin, 5′-GACTCAAGATGATTCCCTTT-3′ (forward) and 5′-GGTGCAAAGTAAGTGAAGGA-3′ (reverse); β-actin, 5′-GGCCACGGCTGCTTC-3′ (forward), 5′GTTGGCGTACAGGTCTTTGC-3′ (reverse). Real-time RT-PCR for periostin and β-actin was performed in parallel and in triplicate per sample, using an iCycler iQ Multi-Color Real Time PCR Detection System (Bio-Rad Laboratories; Hercules, CA) and the following protocol: 50C for 2 min, 95C for 15 min, and 45 cycles at 94C for 30 sec, 60C for 30 sec, and 72C for 30 sec. PCR was performed in a 50-μl reaction mixture containing 25 μl of Platinum SYBR Green qPCR SuperMix-UDG (Invitrogen; Carlsbad, CA), 2.5 μl of forward and reverse primer, 1 μl of each cDNA sample, and 19 μl of ddH_2O. The relative ratio of expression of periostin and β-actin are shown as mean ± SEM.

Proliferation Assay

Proliferation assay was performed using Cell Counting Kit-8 (CCK-8; Dojindo Laboratories, Kumamoto, Japan), a variant MTT assay kit, as the technical manual described with the supplementation of a final concentration of 0.1% BSA and either recombinant human periostin (Biovendor; Heidelberg, Germany) dissolved in PBS or equal amounts of PBS without periostin.

Three-dimensional Co-culture With Cancer Cells and Fibroblasts for the Colony Formation Assay

Collagen gel matrix was prepared using a type I collagen culture kit (Cellmatrix; Nitta Gelatin, Osaka, Japan). HCT116 and either primary-cultured lung fibroblasts derived from periostin$^{+/+}$ and periostin$^{-/-}$ mice or NIH3T3 with transfection of periostin or EGFP at each final concentration of 1×10^6/ml were mixed with chilled reconstituted collagen, and 1 ml of the mixture was pored into a 12-well culture plate and allowed to gel at 37C for 30 min. The next day, the matrix was detached from the bottom of the dish and floated below the surface of the medium. Floating collagen gel culture was conducted for 2 weeks. After that, 10% phosphate-buffered formalin–fixed and paraffin-embedded sections were studied with hematoxylin and eosin stain. Photographs of >36 focuses of high-power fields (HPFs) at random were taken, and each colony area was squared using Multi Gauge ver.2.2 software (FUJIFILM; Tokyo, Japan).

Statistical Analysis

All numerical results are shown as the mean ± SEM. The data were evaluated by Mann-Whitney *U* test or Student's *t*-test for statistical comparisons (cut-off for statistical significance, $p<0.05$) using Statview software (SAS Institute Inc.; Cary, NC).

Results

Immunoreactive Periostin in PCFs of Human and Mouse Colon

In normal colorectal mucosa of both humans and mice, periostin immunoreactivity was observed in the stroma surrounding the crypts (Figure 1A), making up the "pericryptal pattern." There was no immunoreactivity

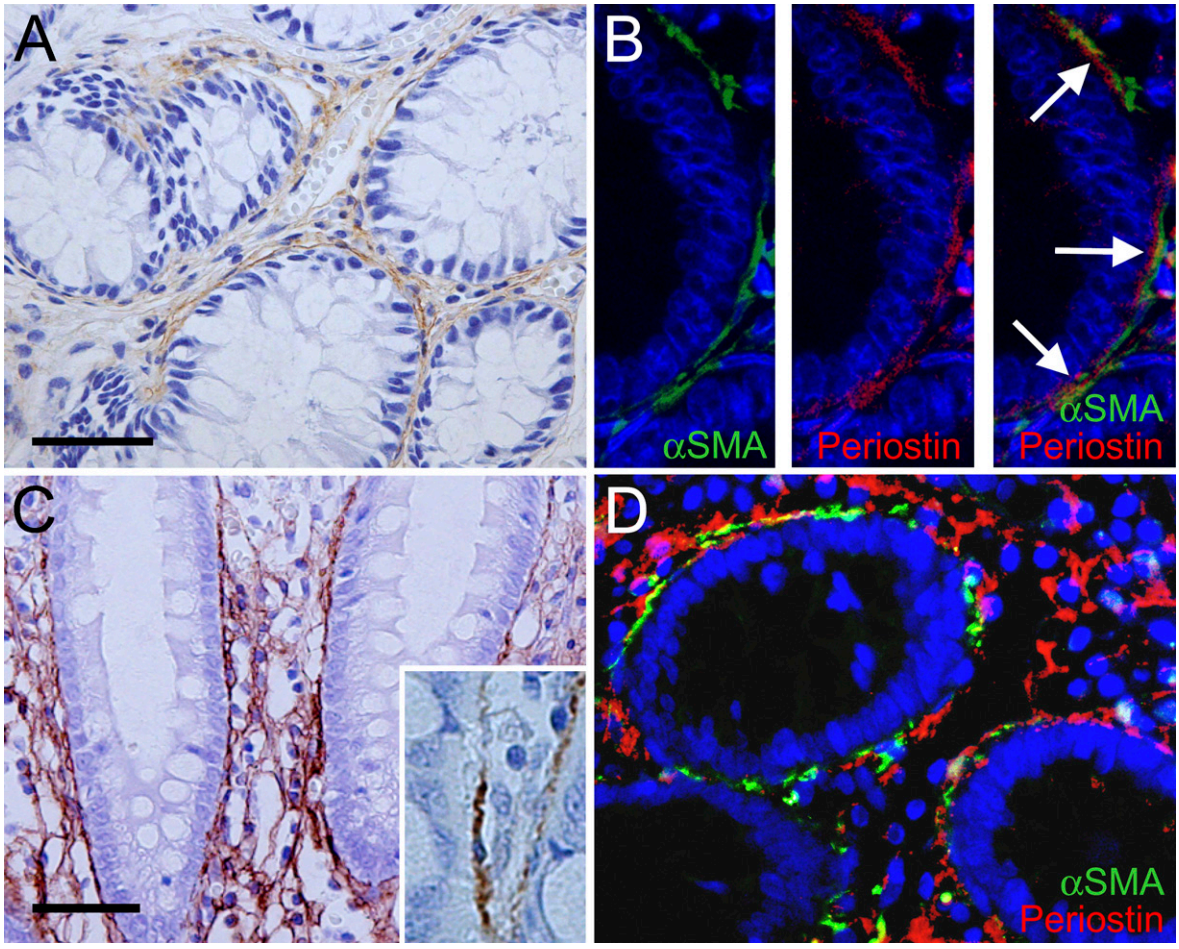

Figure 1 Periostin in non-neoplastic colorectal mucosa. **(A)** Pericryptal pattern of immunoreactive periostin in normal colonic mucosa. Note the linear staining around the crypts. No immunostaining in the epithelial cells. **(B)** Double immunostaining of α smooth muscle actin (αSMA) and periostin to evaluate the topographical relationship of both immunoreactivities. Immunofluorescent staining for αSMA shows the pericryptal fibroblasts (PCFs) rimming the crypts (left). Linear immunofluorescent staining for periostin (center). Merged image showing linear staining of periostin between basement membrane of the crypts and αSMA-positive PCFs (right). Note that condensed deposition of periostin faces αSMA-positive PCF (right; arrows). **(C,D)** Periostin in the inflamed colonic mucosa. **(C)** Mesh pattern of immunoreactive periostin in the colonic mucosa with inflammatory cell infiltration. Mesh-like deposition of immunoreactive periostin in the lamina propria in addition to the pericryptal pattern (inset, high-power magnification showing PCFs). **(D)** Merged image of the double immunofluorescent staining for αSMA and periostin in ulcerative colitis. Note the mesh pattern of periostin in the lamina propria without accompaniment of αSMA-positive cells. Bar = 50 μm.

in the epithelial cells of the colonic crypts or other mesenchymal cells, except for vascular smooth muscle cells. Immunofluorescent double staining for periostin and αSMA (Figure 1B) showed a close approximation of periostin immunoreactivity to αSMA-positive cells, which represent the PCFs. Importantly, periostin deposition was present outside of the basement membrane and frequently faced the αSMA-positive PCFs (Figure 1B).

In the inflammatory condition such as ulcerative colitis, the intensity of the pericryptal pattern of periostin immunoreactivity became stronger; besides the linear immunoreactive material, a mesh pattern was observed throughout the lamina propria (Figures 1C and 1D).

Immunoelectron microscopy of the mouse colonic mucosa (Figure 2) showed the localization of immunoreactivity for periostin. Immunoreactive material was predominantly identified in the narrow space between the PCF and basement membrane, and it mainly delineated the surface of the cytoplasm of PCFs (Figure 2B). There was a small amount of immunoreactive material within the cytoplasm of the PCF, but it was difficult to localize it precisely at the subcellular organella. On the other hand, there was no immunoreactivity identified within the cytoplasm of the epithelial cells. Thus, these findings indicate that PCFs primarily secrete periostin outside to the interstitium, resulting in a pericryptal pattern in the

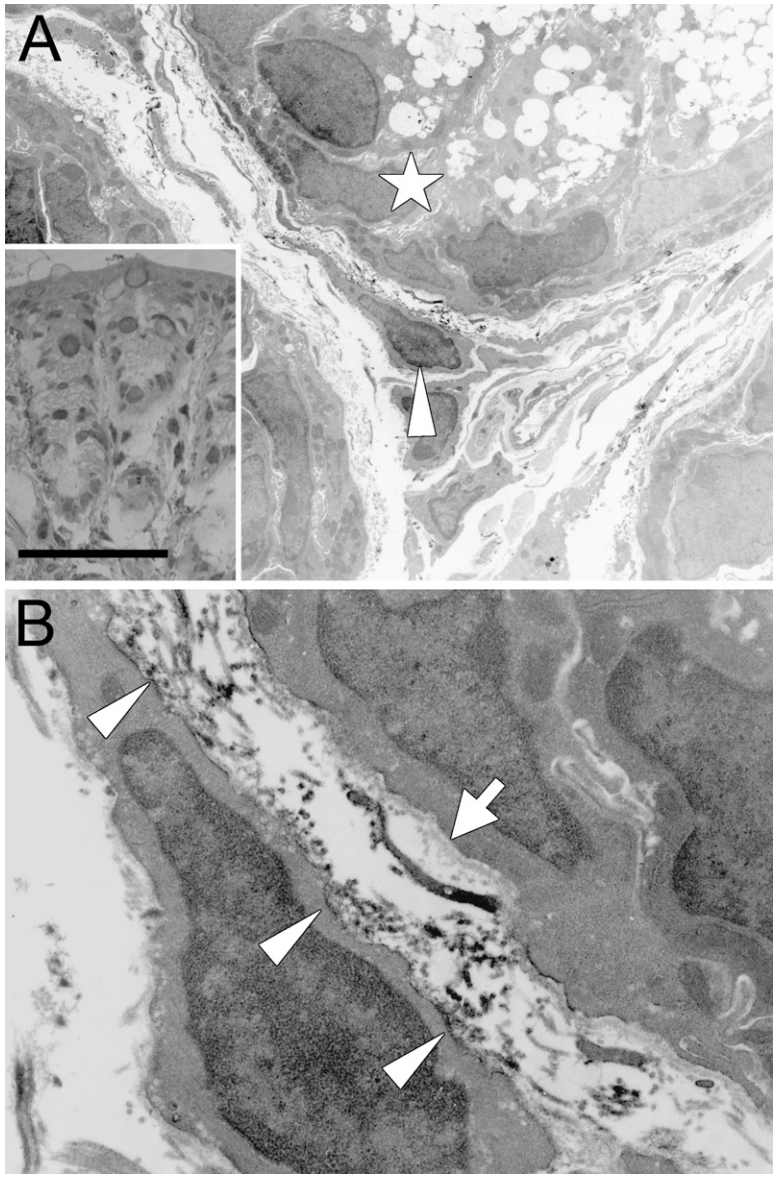

Figure 2 Immunoelectron microscopy of periostin in normal colonic mucosa of the mouse. (**A**) Immunoelectron microscopy of the colonic mucosa of the mouse (arrowhead, PCF; star, colorectal crypt). Note the pericryptal pattern of immunoreactive periostin in the semithin section counterstained with toluidine blue. (**B**) Higher magnification of **A**. Electron dense materials, corresponding to the immunoreactive material, are admitted predominantly in the narrow space between the basement membrane (arrow) and PCF. Immunoreactivity is also observed at the cytoplasmic membrane of the PCF (arrowheads). Bar = 25 μm.

non-neoplastic colorectal mucosa at the light microscopic level.

Dynamics of Periostin Deposition in Relation to the PCF in Pathological Conditions

It is known that the number of PCFs is decreased along the adenoma-carcinoma sequence (Yao and Tsuneyoshi 1993; Higaki et al. 1999; Li et al. 1999). Immunoreactive periostin in the stroma, pericryptal pattern was weakened (Figures 3A and 3B) or disappeared in the adenoma component and completely disappeared in the adenocarcinoma component (Figures 3C and 3D). On immunofluorescence double staining, the amount of periostin immunoreactivity was decreased, and its intensity became weak in the adenoma, even when the number of αSMA-positive cells seemed to be similar to that in normal or hyperplastic mucosa (Figure 3E). Thus, semiquantitative comparative evaluation of periostin and αSMA immunoreactivity showed that the decrease of pericryptal immunoreactivity of periostin precedes the decrease of PCFs along the adenoma-carcinoma sequence (Table 1; Figure 3F).

Immunoreactive Periostin in Cancer-associated Fibroblasts

Periostin immunoreactivity was observed again at the stroma of the early invasive cancer (Figure 3G). The immunoreactive material showed a fibrillar shape, but the intensity was relatively weak and confined to the invasive front. When the carcinoma further

The Journal of Histochemistry & Cytochemistry

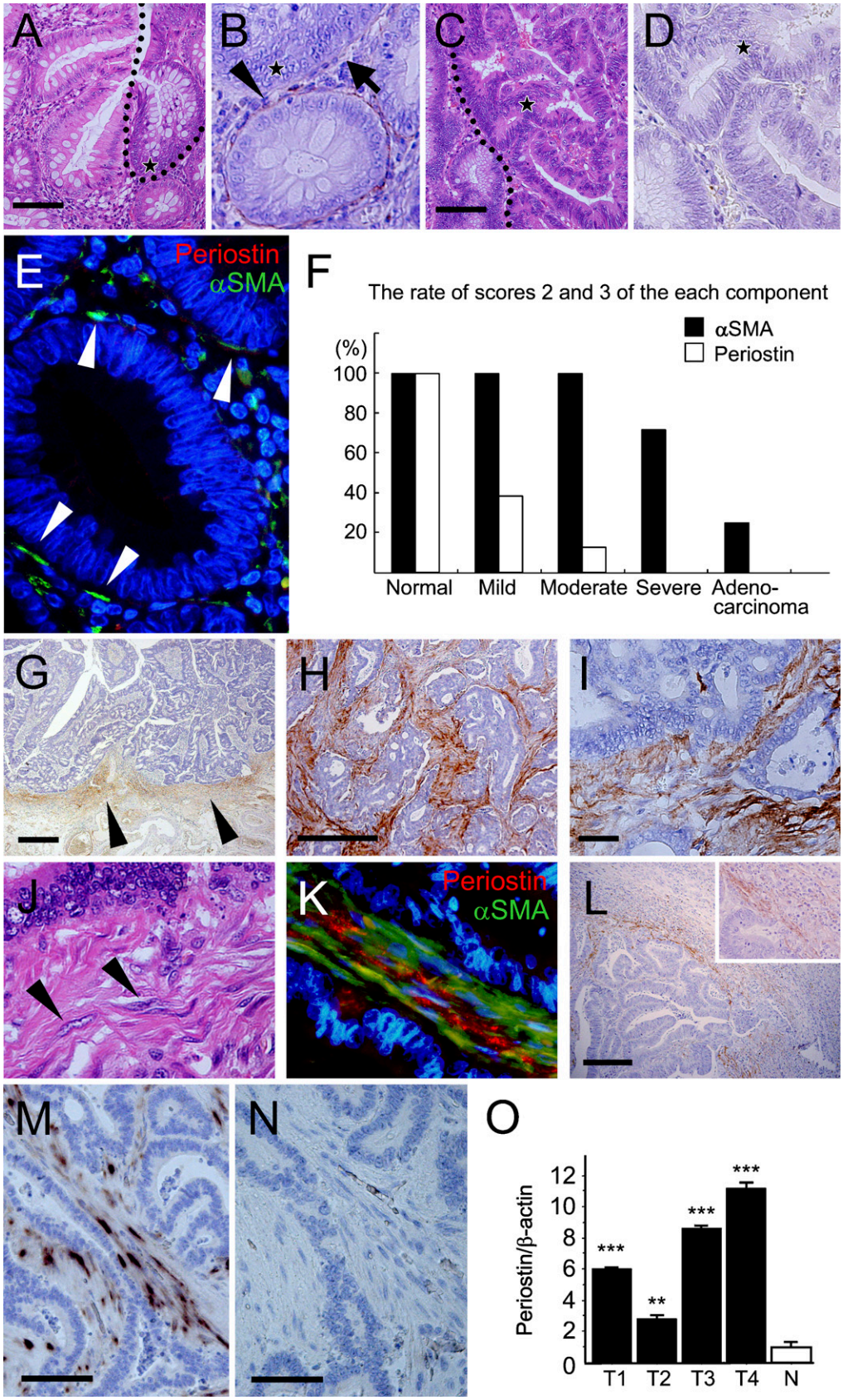
A
B
C
D
E
Periostin
αSMA
F
The rate of scores 2 and 3 of the each component
αSMA
Periostin
(%)
100
80
60
40
20
Normal
Mild
Moderate
Severe
Adeno-carcinoma
G
H
I
J
K
Periostin
αSMA
L
M
N
O
Periostin/β-actin
12
10
8
6
4
2
0
***
**
***
***
T1
T2
T3
T4
N

Table 1 Periostin deposition and αSMA-expressing cells in normal and neoplastic colon

Histology	No. of lesions	Prevalence of gland-expressing periostin				Prevalence of gland-expressing αSMA			
		Score 0 (<10%)	Score 1 (10–49%)	Score 2 (50–80%)	Score 3 (>80%)	Score 0 (<10%)	Score 1 (10–49%)	Score 2 (50–80%)	Score 3 (>80%)
Non-neoplastic colonic crypt	16	0	0	6	10	0	0	0	16
Cancer in adenoma	16								
Adenoma component	16								
Mild	13	3	5	4	1	0	0	0	13
Moderate	16	10	4	1	1	0	0	0	16
Severe	14	12	2	0	0	1	3	3	7
Carcinoma component	16	16	0	0	0	5	7	2	2

αSMA, α smooth muscle actin.

invaded beyond the proper muscles, the stroma integrated within the carcinoma exhibited strong periostin immunoreactivity (Figures 3H and 3I). It became strong and dense compared with immunoreactivity observed in early invasive carcinoma. There were many fibroblastic cells with comparatively plump nuclei within the area showing periostin immunoreactivity (Figure 3J). No staining was observed in carcinoma cells. These findings were highly reproducible; the intensity and localization of immunoreactive periostin did not change by size, grade, or type of carcinoma.

Fibroblasts in cancer stroma, showing characteristics of myofibroblasts, are frequently called CAFs, and one of the well-used immunohistochemical markers for CAF is αSMA, similar to PCFs. The immunofluorescent double staining for αSMA and periostin in advanced invasive cancer (Figure 3K) showed that fibroblast immunoreactive for αSMA appeared in the cancer stroma, and immunoreactive periostin was observed around these cells.

In the metastatic carcinoma of the liver, periostin immunoreactivity was observed in the capsular stroma (Figure 3L). There was little periostin immunoreactivity in normal liver tissue, including the portal areas.

Evaluation of Periostin mRNA Expression by ISH and RT-PCR

To evaluate periostin expression at the mRNA level, ISH was applied to the representative sections of normal and neoplastic colon with antisense (Figure 3M) and sense probes (Figure 3N). There were positive signals of periostin mRNA in the cytoplasm of fibroblastic cells in the stroma of the invasive carcinomas (Figure 3M). No signal was observed in the carcinoma cells. Thus, the finding confirmed that periostin was expressed in CAFs but not in neoplastic epithelial cells.

Quantitative evaluation of mRNA of periostin was performed by real-time RT-PCR in normal colonic mucosa and carcinoma tissues. The amount of periostin mRNA in normal tissue was apparently lower than that in colorectal carcinomas (Figure 3O).

Figure 3 Periostin in adenoma and carcinoma of the colon. (**A–F**) Assessment of periostin expression in each component of cancer in adenoma. (**A**) Border area between non-neoplastic colorectal mucosa and adenoma [dotted line; hematoxylin and eosin (H&E)]. (**B**) Periostin immunohistochemistry of the adenoma component in **A** (star, same point at the star in **A**). Note marked decrease of periostin deposition in the pericryptal region of the adenomatous glands (arrow), in contrast to the preserving of pericryptal pattern in the normal crypts at the border (arrowhead). (**C**) Border area between adenoma and adenocarcinoma (dotted line; H&E). (**D**) Periostin immunohistochemistry of the carcinoma component in **C**, showing complete absence of periostin deposition (star, same point at the star in **C**). (**E**) Double immunostaining for αSMA and periostin in the adenoma. αSMA-positive PCFs are present just beneath the adenoma glands (arrowheads), but immunoreactive periostin is scant. (**F**) Semiquantitative evaluation of periostin and αSMA immunoreactivity relative to the glands of normal and neoplastic colon. The population of positive crypts or glands was scored in four groups according to prevalence: score 0, <10%; score 1, 10–49%; score 2, 50–80%; and score 3, >80%. Scores 2 and 3 are presented in the closed column for αSMA and in the open column for periostin. (**G–N**) Periostin in the invasive and metastatic colorectal carcinoma. (**G**) Periostin at the invasive front of the colorectal carcinoma at its early stage (arrowheads). (**H,I**) Periostin in invasive colorectal carcinoma. (**H**) Infiltrating pattern of periostin deposition in cancer stroma. (**I**) High-power magnification of **H**. No immunoreactivity was identified in the carcinoma cells. (**J**) H&E staining of the corresponding region to **I**. Mesenchymal cells showing spindle-shaped and plump nuclei, morphologically myofibroblasts, within the cancer stroma (arrowheads). (**K**) Immunofluorescent double staining for αSMA and periostin in advanced invasive colorectal cancer showing several portions of colocalization. (**L**) Periostin in the metastatic carcinoma in the liver. Periostin deposition at the capsule of metastatic carcinoma. Note no immunoreactivity in the carcinoma cells or in the normal liver. (Inset) Higher magnification showing fibroblasts within the periostin deposition and those without association of deposition. (**M–O**) Evaluation of periostin mRNA expression in neoplastic and non-neoplastic colon by ISH and real-time RT-PCR. (**M**) ISH of periostin mRNA in colorectal carcinoma. Positive signals were observed in the fibroblastic cells in cancer stroma, whereas no signal was observed in cancer cells. (**N**) No signal was observed in the negative control using sense probe. (**O**) Quantitative real-time RT-PCR analysis of periostin mRNA in neoplastic (T1–T4) and non-neoplastic (N) colon. Statistically significant overexpression was shown compared with the normal colonic tissue (**p<0.01, ***p<0.001). Bars: **A,C,G,H,L** = 500 μm; **I** = 25 μm; **M,N** = 100 μm.

Epithelial Proliferation and Periostin in Normal and Neoplastic Colon

To obtain an insight on the function of periostin produced by PCFs, we performed histological analysis of colon crypts in periostin$^{-/-}$ and periostin$^{+/+}$ mice. There was no significant difference in the number of epithelial cells or PCFs per crypt and the distribution pattern of PCFs between periostin$^{-/-}$ mice and periostin$^{+/+}$ mice (data not shown). PCFs in periostin$^{-/-}$ mice also showed immunoreactivity for αSMA. There was also no difference in the thickness of lamina propria between them. However, the number of Ki-67–positive epithelial cells per crypt was significantly decreased in periostin$^{-/-}$ mice (25.32 ± 8.29/crypt) compared with that in periostin$^{+/+}$ mice (43.04 ± 12.38/crypt) (Figure 4A). Immunohistochemical study for single-strand DNA was also performed to examine the levels of apoptosis, and there was no significant difference in the number of apoptotic cells per crypt between periostin$^{-/-}$ mice (0.13 ± 0.08/crypt) and periostin$^{+/+}$ mice (0.07 ± 0.02/crypt).

To further extend this observation to the neoplastic colon, we evaluated the proliferative effect of periostin on human cancer cells, HCT116, using a proliferation assay with human recombinant periostin. The proliferation of HCT116 cells showed a significant increase in periostin-supplemented conditions at 100 ng/ml after 6 hr of incubation (Figure 4B). The proliferation promoting effect was observed at 10 ng/ml and showed significant difference at 50-1000 ng/ml when evaluated at 24 hr of incubation (Figure 4C).

Cancer–Stromal Interaction Through Periostin in Type I Collagen Gel Three-dimensional Co-culture

For the assessment of cancer–stromal interaction through periostin produced by fibroblasts, we performed a colony formation assay under the three-dimensional co-culture of HCT116 cells and fibroblasts in type I collagen gel. In HCT116 cells co-cultured with periostin$^{+/+}$ fibroblasts, both colony number and size of HCT116 cells were significantly larger (1.30- and 1.30-fold, respectively) than in the co-culture with

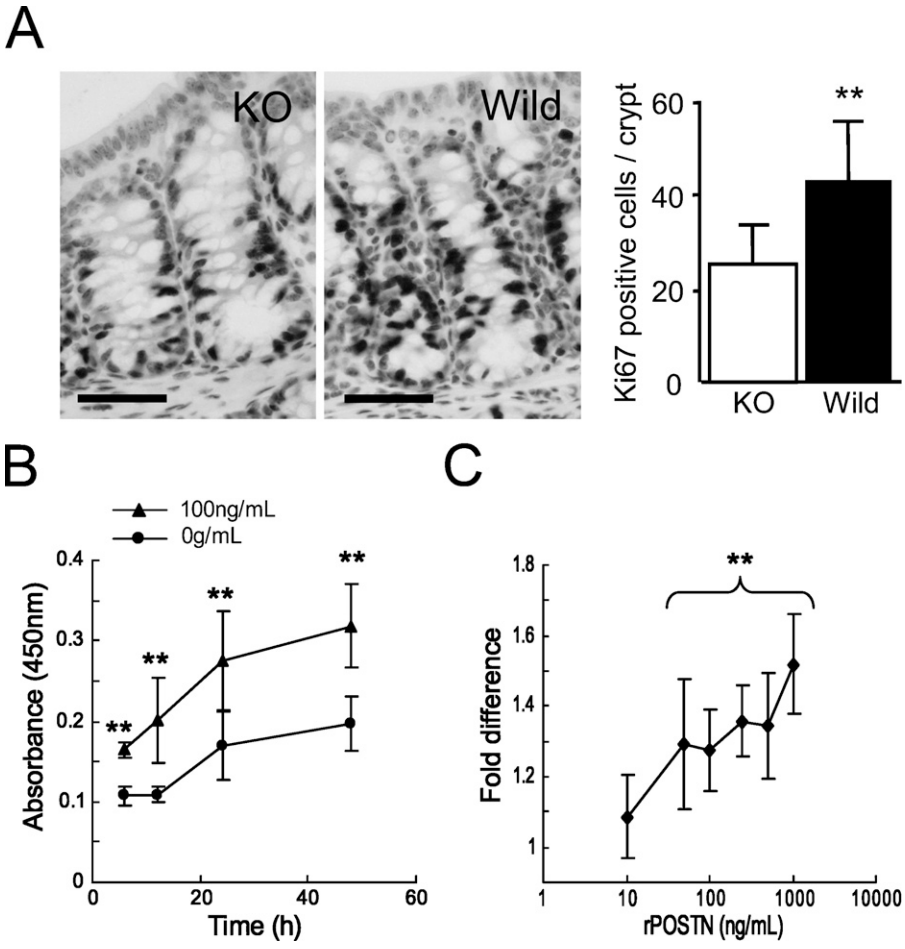

Figure 4 Evaluation of effect of periostin on epithelial proliferation of normal and neoplastic colon. (**A**) Immunohistochemical study of Ki-67 for periostin$^{+/+}$ and periostin$^{-/-}$ mice. The number of Ki-67–positive epithelial cells is larger in the periostin$^{+/+}$ mice than in the periostin$^{-/-}$ mice. There is a statistically significant difference in the number of epithelial cells immunoreactive for Ki-67 per each crypt between periostin$^{+/+}$ and periostin$^{-/-}$ mice (**p<0.01). Ki-67–positive epithelial cells are decreased in periostin$^{-/-}$ mice. (**B**) Proliferation assay of HCT116 supplemented with recombinant periostin (100 ng/ml) in culture medium. The increase of cell number is greater with 100 ng/ml periostin at 6, 12, 24, and 48 hr (**p<0.01). (**C**) Dose response of recombinant periostin. The increase of cell number at 24 hr is represented as fold change compared with the average of negative control. The difference is statistically significant at concentrations >50 ng/ml (**p<0.01) Bar = 50 μm.

periostin$^{-/-}$ fibroblasts. We also tested this experiment using transfectants of the fibroblast cell line, periostin-transfected NIH3T3-secreting periostin and EGFP-transfected NIH3T3 cells. Culture supernatant of the latter NIH3T3 did not show any amount of immunoreactive periostin. As a result, the difference was much more striking (1.48- and 1.54-fold, respectively) when compared between the co-cultures with periostin- and EGFP-transfected NIH3T3 cells (Figure 5; Table 2).

Discussion

Periostin is primarily an extracellular matrix protein, and its function has been intensively studied in non-neoplastic and neoplastic tissues. In this study, we showed that there were several patterns of periostin deposition, such as pericryptal pattern, stromal mesh pattern, and infiltrating pattern, which are shown in Table 3.

Periostin deposition showed a pericryptal pattern in normal colonic mucosa. We showed by immunoelectron microscopy that a specific type of myofibroblasts, PCFs, produces and secretes periostin within the myofibroblastic sheath of the cryptic glands. PCFs in the colon play a fundamental role in the differentiation and in the absorptive function of the crypts (Birchmeier and Birchmeier 1993; Kedinger et al. 1999; Naftalin and Pedley 1999; Powell et al. 1999),

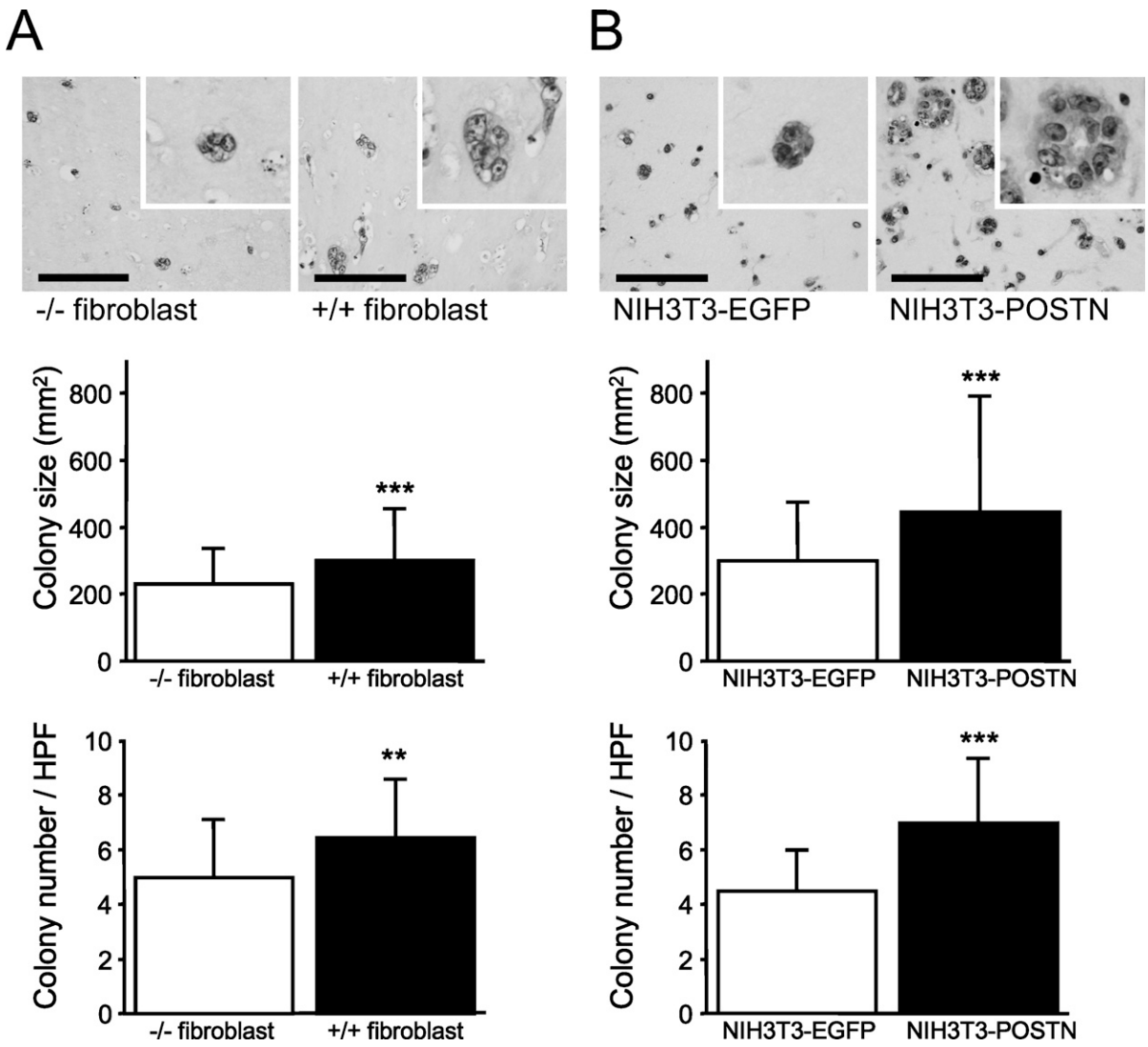

Figure 5 Colony formation assay of HCT116 co-embedded with fibroblasts in type I collagen gel. (**A**) Colony formation assay of HCT116 co-embedded with periostin$^{-/-}$ or periostin$^{+/+}$ primary-cultured fibroblast in type I collagen gel. Both colony size and number are larger in the gel co-embedded with periostin$^{+/+}$ fibroblasts compared with those with periostin$^{-/-}$ fibroblasts (**p<0.01; *** p<0.001). (**B**) Colony formation assay of HCT116 co-embedded with NIH3T3 transfectants. Both colony size and number are larger in the gel co-embedded with periostin-transfected NIH3T3 compared with those with enhanced green fluorescent protein (EGFP)-transfected NIH3T3 (***p<0.001). Bar = 100 μm.

Table 2 Colony size and number of HCT116 cells in three-dimensional co-cultures with fibroblasts

	Colony size (μm^2)	Colony number/HPF
Periostin$^{-/-}$ fibroblast	233.33 ± 107.14[a]	4.97 ± 2.06[b]
Periostin$^{+/+}$ fibroblast	303.57 ± 153.65	6.44 ± 2.11
NIH3T3-EGFP	304.03 ± 175.36[b]	4.50 ± 1.48[b]
NIH3T3-periostin	449.54 ± 350.15	6.94 ± 2.30

[a] $p<0.01$.
[b] $p<0.001$.
HPF, high-power field; EGFP, enhanced green fluorescent protein.

interacting with epithelial cells through a paracrine mechanism by transforming growth factor β (TGFβ), interleukin 6 (IL-6), and leukemia inhibitory factor (Powell et al. 1999; Rockman et al. 2001). We showed the difference of Ki67-labeling indexes in the colonic crypts of periostin$^{-/-}$ and periostin$^{+/+}$ mice, suggesting that periostin also plays a role in regulating epithelial proliferation in normal colon. Furthermore, periostin in the lamina propria in the inflammatory process showing a mesh pattern may play a role in maintaining the integrity of the colonic mucosa. We have previously shown that periostin is fundamental for the tissue repair process of the myocardial infarction (Shimazaki et al. 2008).

Periostin deposition decreased before the number of PCFs became lower in the adenomas and completely disappeared at the stage of intramucosal carcinoma. Periostin is induced by TGFβ, bone morphologic protein-2 (BMP-2), IL-4, or IL-13 in mesenchymal cells (Horiuchi et al. 1999; Ji et al. 2000; Takayama et al. 2006), and it was previously reported that the level of TGFβ and BMP-2 was lower or lost in adenoma-bearing mucosa (Kushiyama et al. 2000), in microadenomas of a mouse model of familial adenomatous polyposis (FAP) (Oshima et al. 1997), and in adenomas of patients with FAP (Hardwick et al. 2004). Thus, it is possible that periostin secretion decreases from PCFs, before PCFs decrease in the adenoma. The finding of periostin decrease heralds the neoplastic growth of colonic epithelial cells and may be useful for pathological diagnosis of the neoplastic change of the epithelial cells of the colon.

There has been controversy regarding the localization of periostin in neoplastic tissues. In this study, the primary cells to produce and secrete periostin are the fibroblastic cells in the interstitium of the carcinoma, i.e., CAFs, which have characteristics of myofibroblasts (Orimo et al. 2005). As for the results of ISH, Baril et al. (2007) showed mRNA of periostin in cancer cells in pancreatic cancer. In contrast, Sasaki et al. (2001,2003) observed weak signals in the carcinoma cells of lung cancers (Sasaki et al. 2001) and breast cancers (Sasaki et al. 2003), and we recently observed that the signals were non-existent in pancreatic cancer (Fukushima et al. in press). According to Erkan et al. (2007), it is the stellate cells that produced periostin in pancreatic cancer. We have no definite explanation for these differences at present, but we frequently observed that endogenous alkaline phosphatase activity in the pancreatic acinar cells disturbs the tissue localization when the alkaline phosphatase method is used for visualization of the signals in the pancreas. Nevertheless, because periostin-transfected carcinoma cells facilitates its motility and metastasis, the induction of periostin in the CAFs was suggested to serve in the growth and development of the carcinomas in a paracrine loop. In this study, recombinant periostin accelerated the growth of HCT116. Both colony size and number of HCT116 cells were significantly larger when cultured with periostin-producing fibroblasts than with non-producing ones in a three-dimensional co-culture system. The fibroblasts used in the study were not derived from the colon, and therefore, the experimental condition was not a true recapitulation of the colon carcinoma. However, these facts strongly suggest that the growth of cancer cells is promoted by periostin through the paracrine route from the coexisting fibroblasts.

Table 3 Pattern of periostin distribution in the normal and neoplastic colon

	Mesenchymal cell expression			
	Pericryptal pattern	Stromal mesh pattern	Stromal infiltrating pattern	Epithelial/cancer cell expression
Non-neoplastic mucosa				
Normal mucosa	+	+/−	−	−
Inflammatory lesion	++	++	−	−
Neoplasm				
Adenoma	+/−	−	−	−
Adenocarcinoma				
Non-invasive	−	−	−	−
Early invasive	−	−	+	−
Advanced invasive	−	−	++	−

++, Strong expression; +, expression; +/−, weak expression; −, no expression.

In conclusion, periostin is a matrix protein secreted by both PCFs and CAFs. PCF–periostin and CAF–periostin may have a similar function, although their regulation is different; the former is regulated by the integrity of the concrete structure of pericryptal sheath, and the latter is unregulated at the invasive site of the stroma of the carcinoma.

Acknowledgments

This work was supported by Grants-in-Aid from Ministry of Education, Culture, Sports, Science and Technology or Japan Society for the Promotion of Science and in part by grants from The Yasuda Medical Foundation to Y.K. No conflicts of interest were declared.

We thank Dr. H. Niwa (RIKEN Center for Developmental Biology, Kobe, Japan) for kind provision of pCAGIPuro vector and M. Fujiwara, K. Sakuma, H. Yamamura, and A. Ogiwara (Department of Pathology and Diagnostic Pathology, Graduate School of Medicine, The University of Tokyo) for technical support.

Literature Cited

Bao S, Ouyang G, Bai X, Huang Z, Ma C, Liu M, Shao R, et al. (2004) Periostin potently promotes metastatic growth of colon cancer by augmenting cell survival via the Akt/PKB pathway. Cancer Cell 5:329–339

Baril P, Gangeswaran R, Mahon PC, Caulee K, Kocher HM, Harada T, Zhu M, et al. (2007) Periostin promotes invasiveness and resistance of pancreatic cancer cells to hypoxia-induced cell death: role of the beta4 integrin and the PI3k pathway. Oncogene 26: 2082–2094

Birchmeier C, Birchmeier W (1993) Molecular aspects of mesenchymal-epithelial interactions. Annu Rev Cell Biol 9:511–540

Erkan M, Kleeff J, Gorbachevski A, Reiser C, Mitkus T, Esposito I, Giese T, et al. (2007) Periostin creates a tumor-supportive microenvironment in the pancreas by sustaining fibrogenic stellate cell activity. Gastroenterology 132:1447–1464

Fukushima N, Kikuchi Y, Nishiyama T, Kudo A, Fukayama M (In Press) Periostin deposition in the stroma of invasive and intraductal neoplasms of the pancreas. Mod Pathol

Gillan L, Matei D, Fishman DA, Gerbin CS, Karlan BY, Chang DD (2002) Periostin secreted by epithelial ovarian carcinoma is a ligand for alpha(V)beta(3) and alpha(V)beta(5) integrins and promotes cell motility. Cancer Res 62:5358–5364

Grigoriadis A, Mackay A, Reis Filho JS, Steele D, Iseli C, Stevenson BJ, Jongeneel CV, et al. (2006) Establishment of the epithelial-specific transcriptome of normal and malignant human breast cells based on MPSS and array expression data. Breast Cancer Res 8:R56

Hardwick JC, Van Den Brink GR, Bleuming SA, Ballester I, Van Den Brande JM, Keller JJ, Offerhaus GJ, et al. (2004) Bone morphogenetic protein 2 is expressed by, and acts upon, mature epithelial cells in the colon. Gastroenterology 126:111–121

Higaki S, Tada M, Nishiaki M, Mitani M, Yanai H, Okita K (1999) Immunohistological study to determine the presence of pericryptal myofibroblasts and basement membrane in colorectal epithelial tumors. J Gastroenterol 34:215–220

Hirose Y, Suzuki H, Amizuka N, Shimomura J, Kawano Y, Nozawa-Inoue K, Kudo A, et al. (2003) Immunohistochemical Localization of Periostin in Developing Long Bones of Mice. Biomed Res 24:31–37

Horiuchi K, Amizuka N, Takeshita S, Takamatsu H, Katsuura M, Ozawa H, Toyama Y, et al. (1999) Identification and characterization of a novel protein, periostin, with restricted expression to periosteum and periodontal ligament and increased expression by transforming growth factor beta. J Bone Miner Res 14: 1239–1249

Japanese Society for Cancer of the Colon and Rectum (2006) General Rules for Clinical and Pathological Studies on Cancer of the Colon, Rectum and Anus. 7th ed. Tokyo, Kanehara

Ji X, Chen D, Xu C, Harris SE, Mundy GR, Yoneda T (2000) Patterns of gene expression associated with BMP-2-induced osteoblast and adipocyte differentiation of mesenchymal progenitor cell 3T3–F442A. J Bone Miner Metab 18:132–139

Kedinger M, Freund JN, Launary JF, Simon-Assmann P (1999) Intestinal development and differentiation. In Sanderson IR, Walker WA, eds. Development of the Gastrointestinal Tract. London, BC Decker, 83–102

Kii I, Amizuka N, Minqi L, Kitajima S, Saga Y, Kudo A (2006) Periostin is an extracellular matrix protein required for eruption of incisors in mice. Biochem Biophys Res Commun 342: 766–772

Kruzynska Frejtag A, Machnicki M, Rogers R, Markwald RR, Conway SJ (2001) Periostin (an osteoblast-specific factor) is expressed within the embryonic mouse heart during valve formation. Mech Dev 103:183–188

Kruzynska Frejtag A, Wang J, Maeda M, Rogers R, Krug E, Hoffman S, Markwald RR, et al. (2004) Periostin is expressed within the developing teeth at the sites of epithelial-mesenchymal interaction. Dev Dyn 229:857–868

Kudo Y, Ogawa I, Kitajima S, Kitagawa M, Kawai H, Gaffney PM, Miyauchi M, et al. (2006) Periostin promotes invasion and anchorage-independent growth in the metastatic process of head and neck cancer. Cancer Res 66:6928–6935

Kushiyama Y, Fukuda R, Suetsugu H, Kazumori H, Ishihara S, Adachi K, Kinoshita Y (2000) Site-dependent production of transforming growth factor beta1 in colonic mucosa: its possible role in tumorigenesis of the colon. J Lab Clin Med 136: 201–208

Li A, Hasui K, Yonezawa S, Tanaka S, Sato E (1999) Immunohistochemical analysis of pericryptal fibroblast sheath and proliferating epithelial cells in human colorectal adenomas and carcinomas with adenoma components. Pathol Int 49:426–434

Naftalin RJ, Pedley KC (1999) Regional crypt function in rat large intestine in relation to fluid absorption and growth of the pericryptal sheath. J Physiol 514:211–227

Norris RA, Damon B, Mironov V, Kasyanov V, Ramamurthi A, Moreno Rodriguez R, Trusk T, et al. (2007) Periostin regulates collagen fibrillogenesis and the biomechanical properties of connective tissues. J Cell Biochem 101:695–711

Orimo A, Gupta PB, Sgroi DC, Arenzana Seisdedos F, Delaunay T, Naeem R, Carey VJ, et al. (2005) Stromal fibroblasts present in invasive human breast carcinomas promote tumor growth and angiogenesis through elevated SDF-1/CXCL12 secretion. Cell 121:335–348

Oshima H, Oshima M, Kobayashi M, Tsutsumi M, Taketo MM (1997) Morphological and molecular processes of polyp formation in Apc(delta716) knockout mice. Cancer Res 57: 1644–1649

Powell DW, Mifflin RC, Valentich JD, Crowe SE, Saada JI, West AB (1999) Myofibroblasts. II. Intestinal subepithelial myofibroblasts. Am J Physiol 277:C183–201

Rockman SP, Demmler K, Roczo N, Cosgriff A, Phillips WA, Thomas RJ, Whitehead RH (2001) Expression of interleukin-6, leukemia inhibitory factor and their receptors by colonic epithelium and pericryptal fibroblasts. J Gastroenterol Hepatol 16: 991–1000

Sasaki H, Dai M, Auclair D, Fukai I, Kiriyama M, Yamakawa Y, Fujii Y, et al. (2001) Serum level of the periostin, a homologue of an insect cell adhesion molecule, as a prognostic marker in nonsmall cell lung carcinomas. Cancer 92:843–848

Sasaki H, Yu CY, Dai M, Tam C, Loda M, Auclair D, Chen LB, et al. (2003) Elevated serum periostin levels in patients with bone metastases from breast but not lung cancer. Breast Cancer Res Treat 77:245–252

Shao R, Bao S, Bai X, Blanchette C, Anderson RM, Dang T, Gishizky ML, et al. (2004) Acquired expression of periostin by human breast cancers promotes tumor angiogenesis through up-regulation of

vascular endothelial growth factor receptor 2 expression. Mol Cell Biol 24:3992–4003

Shimazaki M, Nakamura K, Kii I, Kashima T, Amizuka N, Li M, Saito M, et al. (2008) Periostin is essential for cardiac healing after acute myocardial infarction. J Exp Med 205:295–303

Spradling A, Drummond Barbosa D, Kai T (2001) Stem cells find their niche. Nature 414:98–104

Suzuki H, Amizuka N, Kii I, Kawano Y, Nozawa Inoue K, Suzuki A, Yoshie H, et al. (2004) Immunohistochemical localization of periostin in tooth and its surrounding tissues in mouse mandibles during development. Anat Rec A Discov Mol Cell Evol Biol 281: 1264–1275

Tai IT, Dai M, Chen LB (2005) Periostin induction in tumor cell line explants and inhibition of in vitro cell growth by anti-periostin antibodies. Carcinogenesis 26:908–915

Takayama G, Arima K, Kanaji T, Toda S, Tanaka H, Shoji S, McKenzie AN, et al. (2006) Periostin: a novel component of subepithelial fibrosis of bronchial asthma downstream of IL-4 and IL-13 signals. J Allergy Clin Immunol 118:98–104

Takeshita S, Kikuno R, Tezuka K, Amann E (1993) Osteoblast-specific factor 2: cloning of a putative bone adhesion protein with homology with the insect protein fasciclin I. Biochem J 294:271–278

Yan W, Shao R (2006) Transduction of a mesenchyme-specific gene periostin into 293T cells induces cell invasive activity through epithelial-mesenchymal transformation. J Biol Chem 281: 19700–19708

Yao T, Tsuneyoshi M (1993) Significance of pericryptal fibroblasts in colorectal epithelial tumors: a special reference to the histologic features and growth patterns. Hum Pathol 24:525–533

The Journal of Histochemistry & Cytochemistry